analytical chemistry

Editors' Highlight

pubs.acs.org/ac

A Microelectromechanical Systems-Enabled, Miniature Triple Quadrupole Mass Spectrometer

Steven Wright,*[,†] Andrew Malcolm,[†] Christopher Wright,[†] Shane O'Prey,[†] Edward Crichton,[†] Neil Dash,[†] Richard W. Moseley,[†] Wojciech Zaczek,[†] Peter Edwards,[†] Richard J. Fussell,[‡] and Richard R. A. Syms[§]

[†]Microsaic Systems plc, Woking, Surrey GU21 5BX, U.K.

[‡]Food and Environment Research Agency, Sand Hutton, York YO41 1LZ, U.K.

[§]Department of Electrical and Electronic Engineering, Imperial College, London SW7 2AZ, U.K.

ABSTRACT: Miniaturized mass spectrometers are becoming increasingly capable, enabling the development of many novel field and laboratory applications. However, to date, triple quadrupole tandem mass spectrometers, the workhorses of quantitative analysis, have not been significantly reduced in size. Here, the basis of a field-deployable triple quadrupole is described. The key development is a highly miniaturized ion optical assembly in which a sequence of six microengineered components is employed to generate ions at atmospheric pressure, provide a vacuum interface, effect ion guiding, and perform fragmentation and mass analysis. Despite its small dimensions, the collision cell efficiently fragments precursor ions and yields product ion spectra that are very similar to those recorded using conventional instruments. The miniature triple quadrupole has been used to detect thiabendazole, a common pesticide, in apples at a level of 10 ng/g.

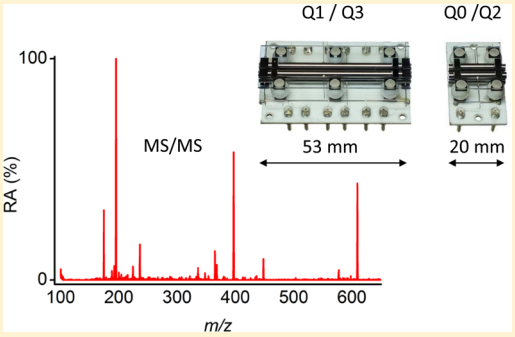

Modern tandem mass spectrometers are able to achieve femtogram detection limits[1−3] but are bulky, expensive, and power-hungry instruments, often operated as central facilities. However, there are important applications that do not demand such high sensitivity and could potentially be better served by smaller, portable instruments. Examples include point-of-care diagnostics, environmental monitoring, security, and drug detection.[4−9] Another potential application is food safety, where there is a need for portable instrumentation capable of rapid, accurate, low-cost detection of pesticides, veterinary drugs, and adulterants.[4,10] The increasing globalization of food supply, high profile food contamination cases, and regional variations in food safety standards have focused attention on the need for testing at all points in the supply chain.[11−13] Given the high volumes of global trade, it is impractical for central facilities to analyze more than a small fraction of the foods reaching consumers. As the levels of contamination significant for human health are relatively high, more widespread, targeted testing could be provided by field-deployable, miniaturized tandem mass spectrometers.

Tandem mass spectrometry involves selection of a precursor ion, fragmentation of the precursor, and analysis of the fragment ions. Selectivity and sensitivity are enhanced, compared with a single-stage instrument, because the fragmentation pathways are characteristic of a particular molecule or class of molecule, and the initial precursor selection rejects matrix components that would otherwise contribute to the chemical noise floor. Analysis may be performed using a tandem-in-space arrangement, such as a triple quadrupole, in which precursor selection, fragmentation, and product ion mass analysis are each performed in separate subsystems. Alternatively, the same processes can all be performed within an ion trap as a tandem-in-time sequence.

The origins of tandem mass spectrometry can be traced to studies of ion−molecule collisions in the 1960s and 1970s.[14] Early systems were based on magnetic sector analyzers.[15] Collisions with a target gas occurred in drift sections or gas cells. Triple quadrupoles were initially developed to study the photofragmentation of selected precursors.[16,17] Apart from their reduced size, a key feature was the use of an intermediate rf-only quadrupole to guide ions through the fragmentation region. Triple quadrupoles evolved into their modern form through the work of Yost and Enke in collaboration with Morrison and co-workers,[18,19] who introduced a collision gas into the rf-only quadrupole. They observed efficient fragmentation and rich, structurally diagnostic product ion spectra at low collision energies. Later, it was shown that fragmentation of selected precursor ions could also be performed in an ion trap by applying an auxiliary ac waveform to induce energetic collisions with the buffer gas.[20]

Previous attempts at miniaturizing tandem mass spectrometers have exclusively involved ion traps.[4−9,21−23] Although the miniaturization of quadrupole filters has been challenging,[24−32] compact single quadrupole instruments have now been developed,[33,34] but so far there have been no attempts to extend the technology to a triple quadrupole format. This is a

Received: December 16, 2014
Accepted: February 23, 2015
Published: February 23, 2015

DOI: 10.1021/acs.analchem.5b00311
Anal. Chem. 2015, 87, 3115−3122

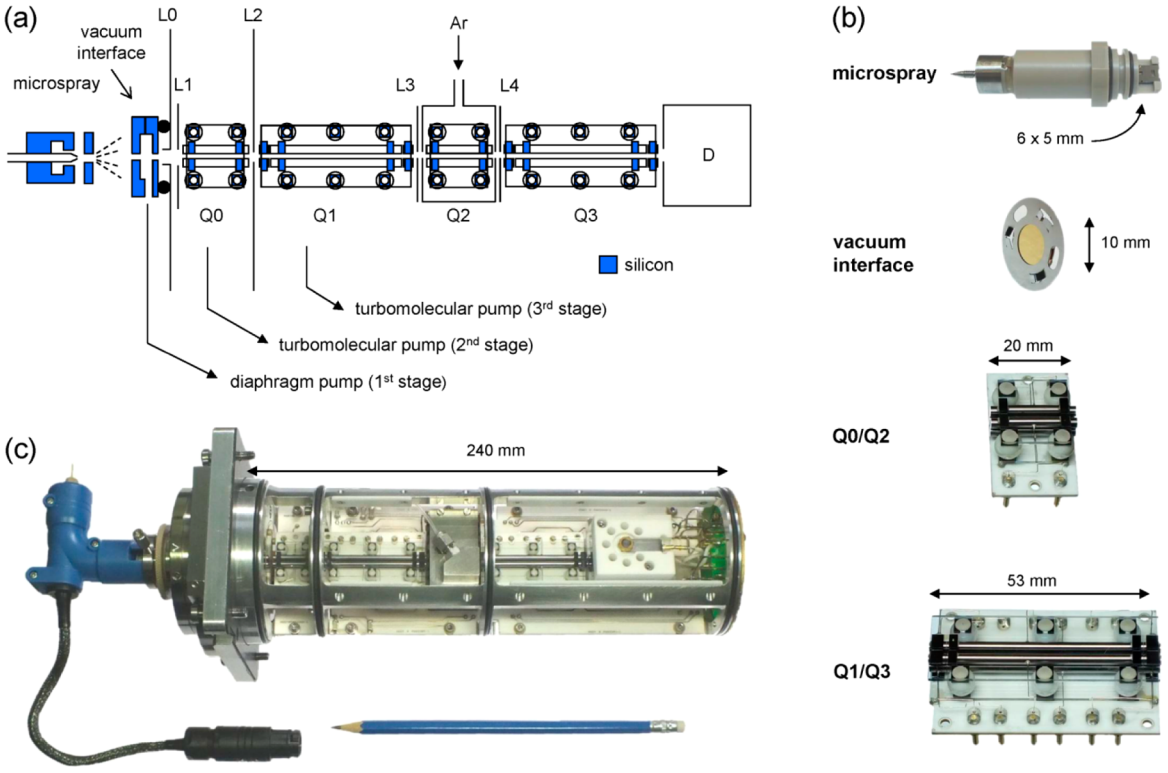

Figure 1. (a) Schematic of the miniaturized ion optics bench (not to scale). Q0 and Q2 are quadrupole ion guides, Q1 and Q3 are quadrupole mass filters, and L0–L4 are electrostatic elements. D is a multiplying detector. (b) Microengineered microspray, vacuum interface, quadrupole ion guide, and quadrupole mass filter. (c) Complete ion optics bench.

potentially significant deficiency, as triple quadrupoles are preferred for some applications.

The relative merits of triple quadrupoles and ion traps have been extensively discussed elsewhere.[35,36] When operated in multiple reaction monitoring (MRM) mode, the duty cycle of triple quadrupoles is similar to that of traps. However, triple quadrupoles achieve better quantitation in chromatography applications, as ion traps must sample quickly changing signals using a variable sampling period to avoid space-charge effects, which leads to poor peak integration. In addition to product ion scans, triple quadrupoles are also able to perform precursor and neutral loss scans. These useful scan modes allow selective detection of similar compounds and may, for example, be used to detect a series of drug metabolites in plasma.[37] Ion traps are unable to execute these scan modes but achieve high selectively by employing multiple fragmentation steps (MS^n). Ion traps are unable to retain product ions with m/z values below the molecular weight cutoff, which is typically one-third of the precursor ion m/z value. This complicates the analysis of some compounds, including tramadol, for example, which yields a diagnostic fragment ion at m/z 58 following selection of the $[M + H]^+$ precursor ion at m/z 264.[38] There is no such limit to the lowest m/z value that can be accessed by triple quadrupoles.

In this paper, we demonstrate a linear triple quadrupole employing microengineered components to carry out all the key steps involved in tandem mass spectrometry, namely, atmospheric pressure ionization, the transfer of ions into vacuum, ion guiding, collision-induced fragmentation, and mass analysis. A total of six microengineered devices are involved, the highest number combined together in any instrument to date. In the following sections, the design, characteristics, and analytical performance of a highly miniaturized ion optical bench, the core of a future compact system, will be described.

EXPERIMENTAL SECTION

Vacuum System and Ion Optics Bench. Figure 1a is a schematic of the ion optics bench. The microspray ion source, vacuum interface, quadrupole ion guides (Q0 and Q2), and quadrupole ion filters (Q1 and Q3) are separate microengineered components. The pneumatically assisted source generates a plume of ions that impinges on the vacuum interface. Ions are drawn into the first vacuum stage through an entrance capillary, together with neutrals. The differentially pumped interface is a flow partitioning device, allowing a fraction of the gas and entrained ions to pass through an exit capillary. Ions transmitted to the second vacuum stage pass first through two electrostatic focusing elements, L0 and L1. The ion beam is then collisionally focused in a 20 mm long quadrupole ion guide, Q0. While most of the ions are retained, neutrals are removed by the second stage pump. A narrow and thermalized ion beam passes through the interquad lens, L2, and into the first of the resolving quadrupoles, Q1. L2 also serves as a pressure bulkhead between the second and third vacuum stages. Precursor ions are selected by Q1 and then enter the collision cell through an aperture, where they undergo energetic collisions with Ar atoms. A 20 mm long quadrupole ion guide, Q2, retains precursor and product ions as they transit the cell. The ions exit through a second aperture and are analyzed by the second mass resolving quadrupole, Q3. The ion detector consists of a conversion dynode and a conventional channeltron.

A 5 L/min diaphragm pump evacuates the vacuum interface, and two turbomolecular pumps backed by a second 5 L/min

DOI: 10.1021/acs.analchem.5b00311
Anal. Chem. 2015, 87, 3115–3122

diaphragm pump evacuate the second and third vacuum stages. During operation, the second stage pressure is 1×10^{-2} Torr while the third stage pressure varies between 3×10^{-5} and 2×10^{-4} Torr, depending on the Ar flow rate. The availability of compact, lightweight pumps has been key to the development of miniature mass spectrometers.[22,33,34] However, since the sensitivity obtained using atmospheric pressure ionization is limited by the amount of gas and entrained ions that can be drawn into vacuum, the limits of detection must reflect their small size. Conventional tandem instruments achieve high sensitivity through the use of bulky floor standing rotary pumps, typically with a speed of 500−1000 L/min and weighing over 40 kg.

Photographs of the ion source, vacuum interface, quadrupole mass filter, and quadrupole ion guide are shown in Figure 1b. These miniaturized components were fabricated using microelectromechanical systems (MEMS) techniques. This generally involves a series of planar processing steps (often silicon-related) that selectively add or remove material. Complex silicon structures can be built-up by etching both sides of the wafer, growing oxide layers, selective metalization, and anodic bonding to glass wafers. As the designs and performance characteristics have been described in detail elsewhere,[32,33,39,40] only a brief overview is given here.

Ions are generated by a low-voltage microspray ion source operating at a flow rate of 0.25−2 μL/min. In conventional systems, the vacuum interface serves as the counter electrode. The device used here incorporates etched silicon features to align a metal spray capillary relative to an integrated counter electrode. As the emitter tip is fixed at the optimum position, no further adjustment is necessary. For convenient handling, the microspray chip is mounted on a polymer cartridge. Nebulizing gas is supplied via a coaxial channel.

The vacuum interface measures 10 mm in diameter and is constructed from two circular silicon dies that are etched so that an internal cavity is formed when they are bonded together back-to-back. Radial channels leading to the perimeter allow differential pumping of the cavity. Ions generated by the microspray are drawn in through a central capillary together with nebulizing gas. Much of the gas and entrained ions is pumped away from the cavity while the remainder passes through an exit capillary and into the second vacuum stage.

The 53 mm long quadrupole mass filter consists of conventionally manufactured cylindrical rods held in a MEMS mounting system. During initial development of this component,[32] the diameter of the rods was 0.65 mm, but this was later increased to approximately 2 mm in order to improve the performance.[33] Other than the addition of postfilters, the initial design has remained essentially unchanged. The four main rods are mounted in pairs on two glass plates that are accurately positioned relative to each other using six ball-and-socket mounts. Etched silicon features bonded to the glass plates support the rods and engage with the spacer balls. The glass plates additionally support sets of short pre- and postfilter rods, which prevent defocusing of the ion trajectories by fringing fields. The 20 mm long ion guides are of a similar construction but do not incorporate pre- and postfilters. Apart from reducing the overall size of the ion optics assembly, there are other benefits associated with miniaturizing the quadrupole mass filters.[24−32] For example, the operating pressure may be increased as the path length of ions in the quadrupole decreases (allowing a smaller turbomolecular pump to be used for the third vacuum stage), and a lower rf voltage is required to achieve a given m/z range.

A photograph of the ion optics bench is shown in Figure 1c. This piston-like structure is accommodated in the circular bore of the vacuum chamber and may be entirely removed as electrical connections are made at the rear with pin and socket connectors. Flat gaskets and O-rings separate the pumping stages when the piston is inserted (the central O-ring provides support only and is not a pressure bulkhead). The microspray cartridge screws into an elbow receiver with mating electrical, fluidic, and gas connectors. This assembly engages with the vacuum interface flange and is held in place by a collar nut. An integrated static fluidic split allows coupling to liquid chromatography systems operating at conventional flow rates. The microengineered vacuum interface is concealed within the stainless steel interface flange but may be accessed without removing the piston assembly. Ceramic boards support the quadrupoles, collision cell, and ion detector. As in earlier systems,[41] electrical connections are provided by metal tracks printed on the boards. Standard push-fit electrical connectors allow modular construction and easy replacement of individual components.

Q2 is located in the stainless steel collision cell between Q1 and Q3. The cell is a two-part assembly comprising a base plate, which is screwed to one of the ceramic boards, and a thin-walled box-like cover measuring 23 mm × 43 mm × 23 mm (L × W × H). Four holes in the base plate allow the ion guide pin connectors to engage with sockets soldered into the ceramic board. Ar is supplied via a gas line routed through the piston frame to a compression fitting on the collision cell lid. Ions enter and exit the cell through 0.7 mm diameter apertures. Lenses are provided immediately before and after the cell to focus the ion beam. For the m/z 195 fragment of reserpine, transmission through Q2 is optimized when the rf amplitude is set at 100 V (0-pk), which corresponds to q (the Mathieu stability parameter) equal to 0.25. There is no provision for an axial electric field in Q2, which is often used to sweep ions out of the collision cell. Several methods can be used to generate an axial field, including use of segmented, tilted, or conical rods.[42−45] A segmented-rod quadrupole of a similar size to Q2 has previously been used to accelerate and fragment ions in a time-of-flight instrument.[46]

In some respects, the ion optics bench is an uneasy marriage of two technologies. High precision is inherent in each of the MEMS components yet they are brought together on an ion optics bench that is fabricated using conventional machine tools. Consequently, some effort must be invested to center each component on the longitudinal axis of the assembly by making manual adjustments. Further use of MEMS technology to cofabricate or self-align multiple ion optical elements offers a route to simplified assembly and improved performance. Minimizing the coupling between the three sets of rf signals and between rf and dc circuits is also an important design consideration. By separating the rf from the dc connections as far as possible, and printing tracks on both sides of the ceramic boards, coupling can be reduced to an acceptable level.

Test System. Testing was undertaken using a breadboard development platform. A commercial single quadrupole (4000 MiD, Microsaic Systems plc, Woking, U.K.) was used as a basis, providing a built-in computer; high voltage supplies for the dynode, channeltron detector, and microspray; a nebulizing gas flow controller; turbomolecular pump controllers; an rf supply for Q3; and dc supplies for the vacuum interface. The vacuum

DOI: 10.1021/acs.analchem.5b00311
Anal. Chem. 2015, 87, 3115−3122

chamber, turbomolecular pumps, and rf amplifiers for Q1 and Q2 were suspended on a frame above the donor chassis. Additional bench power supplies provided dc biases to the prefilters, postfilters, and collision cell. An auxiliary computer controlled the rf amplitudes and main rod biases for Q1 and Q2, while the built-in computer retained control of Q3 scanning and data acquisition. All three rf amplifiers were driven at the same frequency using a signal generator. The frequency was tuned to the resonance frequency of Q3 in combination with its rf amplifier whereas the Q1 and Q2 amplifiers were brought into resonance by high voltage trim capacitors. The power consumption of the vacuum system, rf drives, and doner chassis was 300−400 W, substantially less than the several kilowatts typically demanded by conventional systems.

Preparation of Apple Extracts. Samples were prepared using the QuECheRS (Quick-Easy-Cheap-Rugged-Safe) technique.[47] Organically produced, pesticide-free apples (*malus pumila*) were diced, frozen, and homogenized with a food blender. A 10 g subsample was mixed with 10 mL of acetonitrile, spiked with a known amount of thiabendazole to mimic pesticide contamination, and shaken vigorously for 60 s. Solid reagents (4 g of magnesium sulfate, 1 g of sodium chloride, 0.5 g of sodium citrate dibasic sesquihydrate, 1 g of sodium citrate tribasic dehydrate) were added to adjust the pH and induce phase separation of the organic and aqueous components. After shaking for 60 s, the mixture was centrifuged. The supernatant organic layer was mixed with magnesium sulfate (0.9 g) and a dispersive solid phase extraction agent (0.15 g of PSA) to remove unwanted coextractives. After shaking for 30 s, the mixture was centrifuged again. A sample of the clear acetonitrile solution was then taken for analysis.

Chemicals. Reserpine (≥98%), thiabendazole (99.8%), verapamil hydrochloride (≥99%), formic acid (98%), methanol (HPLC grade), acetonitrile (HPLC grade), and water (HPLC grade) were all purchased from Sigma-Aldrich, Poole, U.K. The QuEChERS extraction reagents were also obtained from Sigma-Aldrich as premixed formulations (Supel QuE citrate (EN) and PSA (EN) tubes). Ar (99.998%) was supplied by Air Liquide UK Ltd., Birmingham, U.K.

RESULTS AND DISCUSSION

Precursor Selection. To achieve high selectivity, it is essential that the desired monoisotopic precursor ion is transmitted by Q1 while other components are rejected. In Figure 2, the spectrum on the left corresponds to mass analysis of the reserpine $[M + H]^+$ ion with the instrument configured as a single quadrupole. The Ar supply to the collision cell was turned off and Q1 was operated in rf-only (all-pass) mode while Q3 was scanned. The monoisotopic ion appears at m/z 609, while the ^{13}C isotope peaks are observed at m/z 610 and m/z 611 with the expected intensities. The spectrum on the right was obtained with the instrument configured as a tandem mass spectrometer. Q1 was operated in mass resolving mode and set to transmit m/z 609 with unit resolution (~0.7 m/z units fwhm) while Q3 was scanned, also with unit resolution. Ar was introduced into the collision cell, but the collision energy was kept low to limit fragmentation. No evidence of m/z 610 or m/z 611 can be seen in the spectrum, indicating that the desired precursor had been correctly isolated by Q1.

Collision Cell. The key parameters governing fragmentation and product ion yields are the collision energy and the target

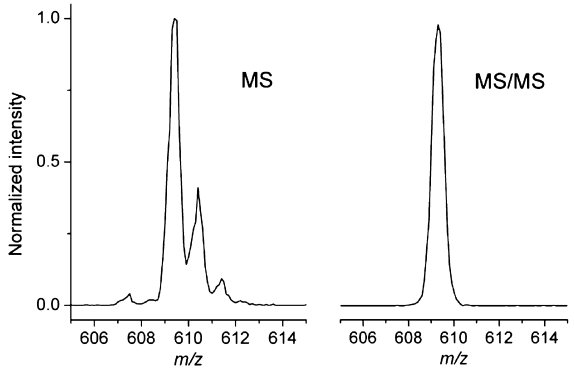

Figure 2. Demonstration of precursor ion selection. The reserpine spectrum on the left was obtained with the instrument configured as a single quadrupole (Q1 in rf-only mode). The spectrum on the right was obtained with the instrument configured as a tandem mass spectrometer (Q1 set to pass m/z 609 with unit resolution).

gas pressure. It is demonstrated below that the miniaturized collision cell yields rich product ion spectra at conventional collision energies and can transmit ions with high efficiency when the gas pressure is optimized.

A series of product ion spectra from the fragmentation of reserpine at collision energies ranging from 20 to 35 eV are shown in Figure 3. Both Q1 and Q3 were operated at unit resolution. At 20 eV, there is little evidence of fragmentation and the spectrum is dominated by the precursor ion at m/z

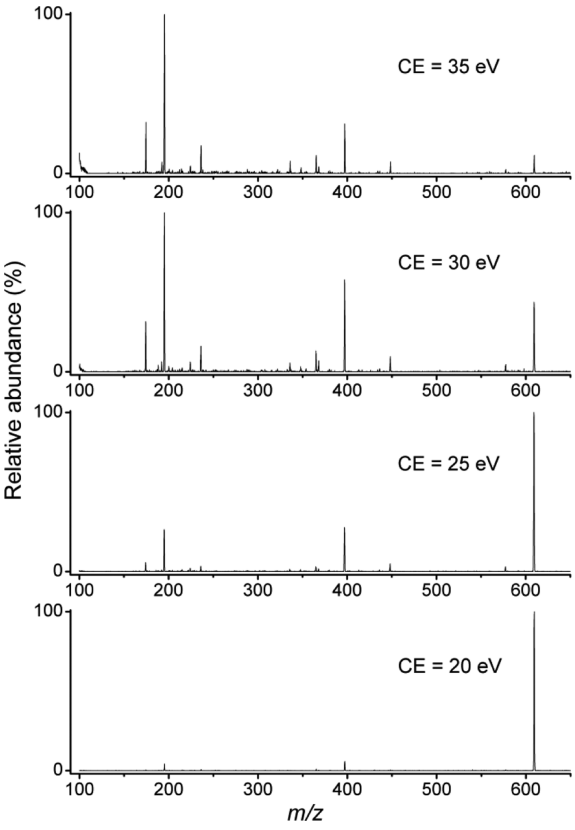

Figure 3. Product ion spectra resulting from the fragmentation of reserpine at collision energies ranging from 20 to 35 eV. Product ions are observed at m/z 174, 195, 236, and 397 when the collision energy (CE) exceeds 20 eV. The spectra have not been centroided or otherwise processed.

DOI: 10.1021/acs.analchem.5b00311
Anal. Chem. 2015, 87, 3115−3122

609. However, at 30 and 35 eV, fragmentation is extensive and prominent product ions are observed at m/z 174, 195, 236, and 397. Essentially identical spectra have been recorded using conventional triple quadrupoles at similar collision energies.[48,49] It should be noted that the low mass product ions appear below one-third of the precursor ion m/z value and would therefore not be seen with an ion trap operating in MS/MS mode.

Figure 4 shows how precursor and product ion intensities depend on the collision cell gas pressure. To simplify the analysis, thiabendazole, which yields only two major product ions, was used. The collision energy was set at 24 eV, as this results in an approximately uniform distribution of precursor and product ions at the optimum pressure. No attempt was made to measure the collision cell pressure directly, as the additional fittings would add considerable complexity. Instead, the pressure was calculated using the relationship $\Delta P = Q/C$, where ΔP is the pressure difference between the collision cell and the surrounding vacuum, C is the combined conductance of the entrance and exit apertures, and Q is the Ar gas flow. Assuming molecular flow (valid for cell pressures less than ~0.1 Torr), the conductance may be calculated using $C = 0.25\nu A$, where A is the area of the apertures, and ν is the average velocity of Ar. Q may be determined from the pressure increase in the third vacuum stage and the known pumping speed of the turbomolecular pump, and ν can be calculated using kinetic theory.

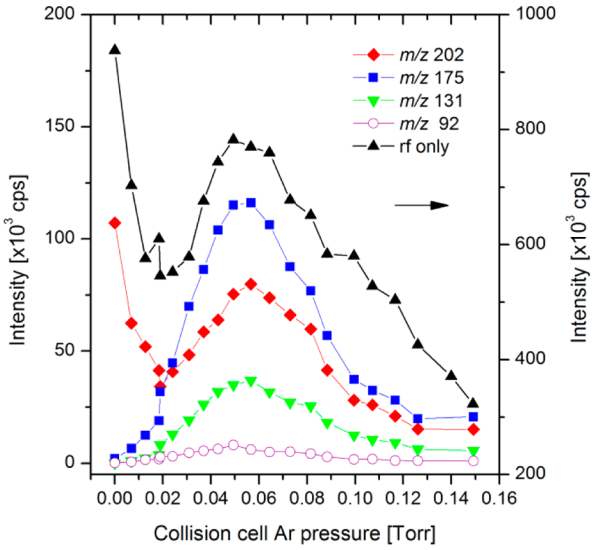

Figure 4. Dependence of thiabendazole precursor and product ion intensities (left axis) on the collision cell Ar pressure. The $[M + H]^+$ ion appears at m/z 202 and major product ions at m/z 131 and 175. Also shown is the signal recorded with Q3 in rf-only mode (right axis), which corresponds to the total ion count. Collisional cooling and fragmentation are optimal at 0.05 Torr.

Also shown in Figure 4 is the signal recorded with Q3 operated in rf-only mode. With the dc components of the drive waveform removed, all ions with $q \leq 0.908$ are simultaneously transmitted and the signal can be taken as a measure of the total ion flux leaving the collision cell. An rf amplitude (0-pk) of 75 V was used for these measurements, and consequently, only ions with $m/z < 40$ were excluded.

When the Ar pressure is increased, the total ion and precursor ion intensities initially decrease sharply, following the Beer–Lambert law, $I = I_0 \exp(-\sigma nL)$, where σ is the collision cross-section, n is the number density, and L is the path length. In this low-pressure regime, ions are scattered and lost from Q2. However, as the pressure is increased further, the precursor ion intensity recovers and the product ion peaks quickly become more intense. This increase in transmitted ion flux, which passes through a maximum at 0.05 Torr, is characteristic of collisional focusing,[49−52] a process by which ions lose kinetic energy through collisions with the target gas. As the ions lose energy, their harmonic oscillations within the pseudopotential well generated by the ion guide become damped, causing accumulation of ions close to the axis. The resulting narrow and thermalized beam is efficiently transmitted through the small exit aperture of the collision cell and is well matched to the acceptance characteristics of Q3, resulting in an increase in signal.

At 0.05 Torr, the collision gas thickness (the product of gas density and the cell length) is 3.2×10^{15} cm^{-2}, close to the value of 4×10^{15} cm^{-2} established as optimum for a collision cell employing a 15 cm long conventional ion guide and Ar as the collision gas.[49] This result suggests that the optimum collision gas thickness may be universal (for a given collision gas), even when the cell length and pressure are changed by an order of magnitude. The same optimum value has also been established for a quadrupole used to guide ions introduced into vacuum,[50] although in this case, nitrogen was used to effect collisional cooling. Two other investigations have reported much higher values. The optimum collision gas thickness for a 40 cm long quadrupole beam cooler in a nuclear physics experiment[53] was 7×10^{16} cm^{-2}, but this high value may be attributable to the use of He rather than Ar as the collision gas (less energy is transferred per collision when the mass of the target is reduced). More intriguing is an investigation of the characteristics of a 7 cm long quadrupole ion guide,[54] which showed that the optimum pressure for transmission of angiotensin III and its fragments is in the range of 0.3–0.5 Torr, equivalent to a collision gas thickness of $0.7–1.1 \times 10^{17}$ cm^{-2}. Although the use of dry air as the buffer accounts for some loss of efficiency (compared with Ar), this value still seems anomalous.

It can be concluded from the rf-only signal that at 0.05 Torr, the total ion flux recovers to 75% of the value measured with no Ar present. Although the transmission is expected to be high at the base pressure, it is unlikely to be 100%, as some of precursor ions are lost through scattering with the residual gas. A previous study has reported efficiencies of 30–50% for a conventional collision cell.[49] However, the calculation was based on resolved peak heights rather than total ion measurements, which convolutes the transmission and filtering characteristics of Q3 with the ability of the collision cell to transmit ions.

Sensitivity and Dynamic Range. Flow injection analysis (FIA) was used to assess sensitivity and dynamic range. A loop injection valve was used to inject 2 μL aliquots of stock reserpine solutions into a solvent stream flowing at 200 μL/min. The fluidic split ratio was set at 300:1. A 70:30:0.1 mixture of acetonitrile, water, and formic acid was used as the carrier solvent and the diluent for stock solutions. The intensity of the m/z 609 →195 transition was monitored with a dwell time of 200 ms and a collision energy of 30 eV. Each signal transient was 3–4 s wide. Figure 5 shows a plot of signal transient area (average of seven injections) against concentration. The detection limit is 5 ng/mL (S/N = 3, peak-to-peak definition)

DOI: 10.1021/acs.analchem.5b00311
Anal. Chem. 2015, 87, 3115–3122

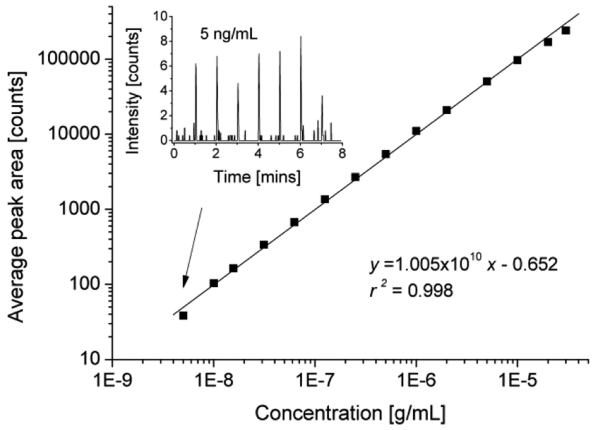

Figure 5. Evaluation of sensitivity and dynamic range by flow injection analysis of reserpine. The limit of detection is 5 ng/mL (10 pg injected), and the response is linear over 4 orders of magnitude.

and the response is linear over 4 orders of magnitude (5 ng/mL to 30 μg/mL). At the detection limit, 10 pg of reserpine was injected but only 30 fg was passed via the split to the mass spectrometer.

Coupling to Liquid Chromatography. There has been considerable progress in ambient ionization techniques and direct analysis protocols that allow mass analysis without chromatographic separation. This is particularly important for field applications, since the overall system size is significantly reduced and sample preparation becomes less onerous. However, at present, the majority of methods, including those relating to food safety, dictate the use of separation prior to mass spectrometry. For field use, a miniaturized triple quadrupole should ideally be coupled to a miniaturized separation stage. However, for initial evaluation, a conventional high-performance liquid chromatography (HPLC) system (1100 series, Agilent, Santa Clara, CA) fitted with an Ascentis Express C18 column (10 cm × 0.46 cm, Sigma-Aldrich) was used.

Figure 6 shows a chromatogram obtained following injection of 1 ng of verapamil. The signal corresponds to the intensity of the m/z 455 → 165 transition (34 eV collision energy), which was monitored with a dwell time of 200 ms. The solvent

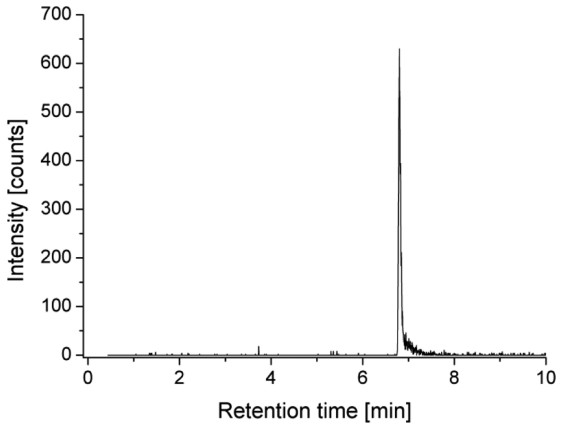

Figure 6. Chromatogram corresponding to 1 ng of verapamil on-column. The intensity of the m/z 455 → 165 transition was monitored at a collision energy of 34 eV. The data have not been smoothed or otherwise processed.

gradient of water (A) and acetonitrile (B), both with 0.1% formic acid, was set such that B = 10% at 0 min, 10% at 2 min, 100% at 9.5 min, 100% at 11.5 min, 10% at 13.5 min, and 10% at 16.5 min. Five consecutive injections yielded peak areas with a relative standard deviation (RSD) of 5.1%. The signal-to-noise ratio is 100:1 using the peak-to-peak definition and 540:1 using the rms definition. Of the 1 ng injected, only 1 pg was passed to the mass spectrometer, as the static split was set at 1000:1 to accommodate a column flow rate of 0.8 mL/min. From the area of the peak in Figure 6, which gives the total number of ion counts at m/z 165 resulting from 1 pg of verapamil in solution, the probability of detection is calculated to be 2×10^{-5}, which is within the range of values reported for conventional instruments.[49,55]

Detection of a Pesticide in Apple. A potential application of a field-deployable triple quadrupole is the monitoring of pesticide residues. To demonstrate this application, the instrument was used to detect and quantify thiabendazole (a common pesticide used to control fungal disease) in apples. Acetonitrile extracts were prepared from whole apples using the QuECheRS technique.

Figure 7a shows MRM chromatograms for the m/z 202 → 175 and m/z 202 → 131 transitions. The intensities were monitored cyclically using a dwell time of 200 ms and a collision energy of 24 eV. The mass spectrometer was coupled to an HPLC as described above, but methanol was used instead of acetonitrile. The gradient was programmed such that B = 10% at 0 min, 10% at 2 min, 100% at 9.5 min, 100% at 11.5 min, 10% at 13.5 min, and 10% at 16.5 min. The samples were diluted with water (1:1) to improve the peak shapes and better match the sample solvent to the initial gradient composition. Five injections were performed for each sample. Distinct peaks are observed for both transitions at a retention time of 6.2 min, even for the 10 ng/g sample. Despite the complex nature of the biological matrix, the noise floor is very low (less than 20 counts/min for the m/z 202 → 175 transition). The peak area repeatability for five consecutive injections, expressed as the RSD, is 5.3% for the 100 ng/g sample and 17.0% for the 10 ng/g sample.

To check the recovery efficiency of the QuECheRS extraction, matrix-matched calibration samples were prepared by adding known amounts of thiabendazole to aliquots of unspiked apple extract. A calibration graph covering the range of interest is shown in Figure 7b. As an internal standard was not used, absolute peak areas rather than peak area ratios are plotted against concentration. Using this calibration, the concentration of thiabendazole in apple spiked at 100 ng/g is determined to be 117 ng/mL. Given that the volume of acetonitrile used was 10 mL, it follows that a total of 1170 ng was present in the final extract. Hence, the calculated recovery is 117%, since 1000 ng was originally added to 10 g of apple homogenate. Values within the range 60−140% are considered to be acceptable.[56]

Biological matrixes are known to cause contamination of vacuum interfaces, resulting in a loss of sensitivity over time. The deposition of involatile matrix components over the surfaces of the vacuum interface leads to the formation of a dielectric layer, which charges up and repels ions. Physical occlusion of the inlet due to accumulation of material on the inner walls also progressively reduces the transmitted ion flux. During the testing described above, 54 injections of apple extract, each of 5 μL, were performed over a period of 2 weeks. A regular check revealed that the sensitivity decreased by 25%

DOI: 10.1021/acs.analchem.5b00311
Anal. Chem. 2015, 87, 3115−3122

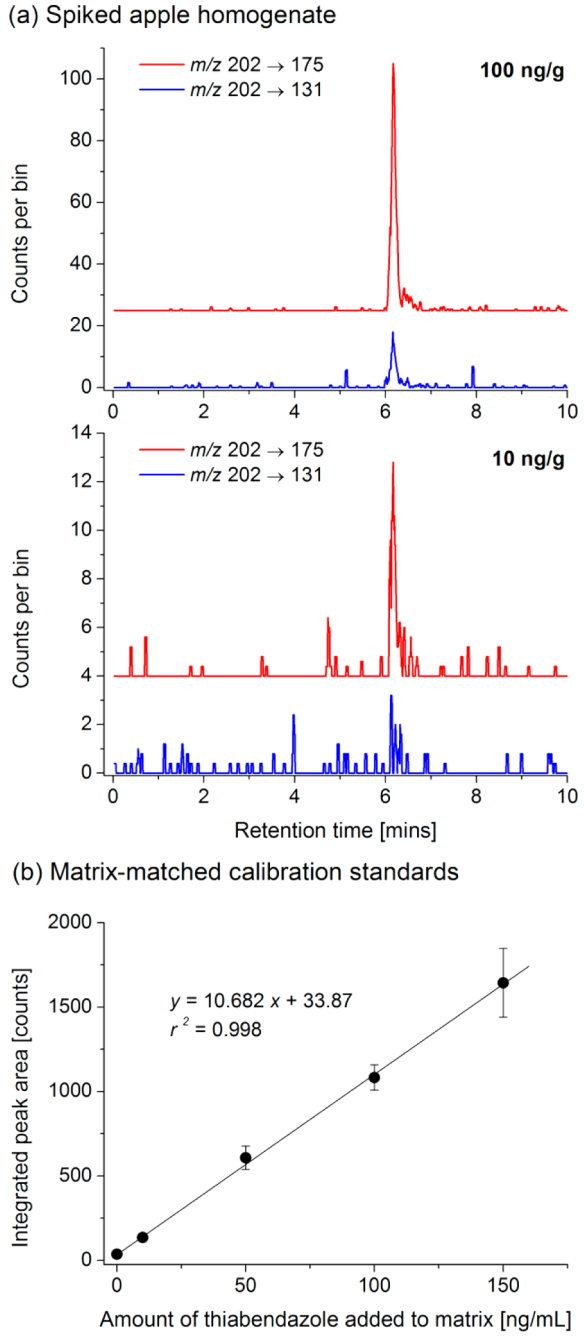

Figure 7. (a) MRM chromatograms corresponding to thiabendazole concentrations of 10 and 100 ng/g in apple homogenate. The m/z 202 → 175 transition is used for quantitation whereas the m/z 202 → 131 transition is used as the qualifier. The data have been smoothed using a five point moving average, and the m/z 202 → 175 chromatograms have been offset to aid presentation. (b) Matrix-matched calibration obtained by adding known amounts of thiabendazole to unspiked apple extract.

during this time. On removal of the vacuum interface component, some light fogging of the originally pristine surface could be seen. This contamination, which is attributed to the deposition of involatile apple extract components, can be removed by immersing the vacuum interface in solvent and applying ultrasonic agitation.

CONCLUSIONS

A miniaturized triple quadrupole constructed using MEMS components has been demonstrated for the first time. The instrument allows precursor ions to be selected with unit resolution and fragmented with high efficiency, yielding rich product ion spectra. The characteristics of the key new feature, a MEMS collision cell, have been investigated. It has been shown that the short length can be compensated for by using a much higher than usual target gas pressure.

One inevitable consequence of miniaturization is reduced sensitivity. Nevertheless, it has been demonstrated that a pesticide can be detected at 10 ng/g in a biological matrix, suggesting that the instrument is potentially suitable for food safety testing. The applications that could be addressed by a field-deployable triple quadrupole should be viewed from the perspective of the complete analytical process, including sample preparation. In many cases, significant analyte enrichment and stripping of matrix components can be achieved through the use of solid phase extraction media, which are often available in formats suitable for field use. Moreover, MEMS technology could be further exploited to recover some of the sensitivity lost as a result of miniaturization. For example, high-density arrays of microfabricated electrospray emitters could provide a means of increasing the ion flux through the vacuum interface.[57,58]

AUTHOR INFORMATION

Corresponding Author

*E-mail: swright@microsaic.com. Phone: +44 1483 751577. Fax: +44 1483 757901.

Notes

The authors declare no competing financial interest.

ACKNOWLEDGMENTS

This work was funded by the European Commission as part of the FP7 Programme (ARROWS project). Helpful discussions with Charles Smith, Consultant, are gratefully acknowledged.

REFERENCES

(1) Thomson, B. *Genet. Eng. Biotechnol. News* **2012**, *32*, 17.
(2) Bayen, S.; Yi, X.; Segovia, E.; Zhou, Z.; Kelly, B. C. *J. Chromatogr. A* **2014**, *1338*, 38−43.
(3) Sun, L.; Li, H.; Willson, K.; Breidinger, S.; Rizk, M. L.; Wenning, L.; Woolf, E. J. *Anal. Chem.* **2012**, *84*, 8614−8621.
(4) Li, L.; Chen, T.-C.; Ren, Y.; Hendricks, P. I.; Cooks, R. G.; Ouyang, Z. *Anal. Chem.* **2014**, *86*, 2909−2916.
(5) Chen, T.-C.; Ouyang, Z. *Anal. Chem.* **2013**, *85*, 1767−1772.
(6) Kumano, S.; Sugiyama, M.; Yamada, M.; Nishimura, K.; Hasegawa, H.; Morokuma, H.; Inoue, H.; Hashimoto, Y. *Anal. Chem.* **2013**, *85*, 5033−5039.
(7) Smith, J. N.; Noll, R. J.; Cooks, R. G. *Rapid Commun. Mass Spectrom.* **2011**, *25*, 1437−1444.
(8) Hendricks, P. I.; Dalgleish, J. K.; Shelley, J. T.; Kirleis, M. A.; McNicholas, M. T.; Chen, T. C.; Chen, C.-H.; Duncan, J. S.; Boudreau, F.; Noll, R. J.; Denton, J. P.; Roach, T. A.; Ouyang, Z.; Cooks, R. G. *Anal. Chem.* **2014**, *86*, 2900−2908.
(9) Wells, J. M.; Roth, M. J.; Keil, A. D.; Grossenbacher, J. W.; Justes, D. R.; Patterson, G. E.; Barket, D. J., Jr. *J. Am. Soc. Mass Spectrom.* **2008**, *19*, 1419−1424.
(10) Krska, R.; Suman, M.; Janssen, H.-G.; Pico, Y.; Nielen, M. *The Analytical Scientist*; ISSN: 2051-4077, Texere Publishing Ltd.: Cheshire, UK, **2013**, *10*, 34−39.
(11) *Ensuring Safe Foods and Medical Products Through Stronger Regulatory Systems Abroad*; Riviere, J. E.; Buckley, G. J., Eds.; The National Academies Press: Washington DC, 2012.

DOI: 10.1021/acs.analchem.5b00311
Anal. Chem. 2015, 87, 3115−3122

(12) Xin, H.; Stone, R. *Science* **2008**, *322*, 1310−1311.
(13) Commission of the European Communities. Commission decision of 20 June 2003 on emergency measures regarding hot chilli and hot chilli products (2003/460/EC), *Off. J. Eur. Union*, L154/114.
(14) Shukla, A. K.; Futrell, J. H. *J. Mass Spectrom.* **2000**, *35*, 1069−1090.
(15) Futrell, J. H.; Miller, C. D. *Rev. Sci. Instrum.* **1966**, *37*, 1521.
(16) McGilvery, D. C.; Morrison, J. D. *J. Chem. Phys.* **1977**, *67*, 368−369.
(17) Vestal, M. L.; Futrell, J. H. *Chem. Phys. Lett.* **1974**, *28*, 559−561.
(18) Yost, R. A.; Enke, C. G. *J. Am. Chem. Soc.* **1978**, *100*, 2274−2275.
(19) Yost, R. A.; Enke, C. G.; McGilvery, D. C.; Smith, D.; Morrison, J. D. *Int. J. Mass Spectrom. Ion Phys.* **1979**, *30*, 127−136.
(20) Louris, J. N.; Cooks, R. G.; Syka, J. E. P.; Kelley, P. E.; Stafford, G. C.; Todd, J. F. J. *Anal. Chem.* **1987**, *59*, 1677−1685.
(21) Laughlin, B. C.; Mulligan, C. C.; Cooks, R. G. *Anal. Chem.* **2005**, *77*, 2928−2939.
(22) Gao, L.; Song, Q.; Patterson, G. E.; Cooks, R. G.; Ouyang, Z. *Anal. Chem.* **2006**, *78*, 5994−6002.
(23) Jiang, D.; Jiang, G.-Y.; Li, X.-X.; Xu, F.-X.; Wang, L.; Ding, L.; Ding, C.-F. *Anal. Chem.* **2013**, *85*, 6041−6046.
(24) Geear, M.; Syms, R. R. A.; Wright, S.; Holmes, A. S. *J. Microelectromech. Syst.* **2005**, *14*, 1156−1166.
(25) Orient, O. J.; Chutjian, A.; Garkanian, V. *Rev. Sci. Instrum.* **1997**, *68*, 1393−1397.
(26) Holkeboer, D. H.; Karandy, T. L.; Currier, F. C.; Frees, L. C.; Ellefson, R. E. *J. Vac. Sci. Technol. A* **1998**, *16*, 1157−1162.
(27) Ferran, R. J.; Boumsellek, S. *J. Vac. Sci. Technol. A* **1996**, *14*, 1258−1265.
(28) Cheung, K.; Velásquez-García, L. F.; Akinwande, A. I. *J. Microelectromech. Syst.* **2010**, *19*, 469−483.
(29) Taylor, S.; Tindall, R. F.; Syms, R. R. A. *J. Vac. Sci. Technol. B* **2001**, *19*, 557−562.
(30) Velásquez-García, L. F.; Cheung, K.; Akinwande, A. I. *J. Microelectromech. Syst.* **2008**, *17*, 1430−1438.
(31) Wright, S.; Syms, R. R. A.; O'Prey, S.; Hong, G.; Holmes, A. S. *J. Am. Soc. Mass Spectrom.* **2009**, *20*, 146−156.
(32) Wright, S.; O'Prey, S.; Syms, R. R. A.; Hong, G.; Holmes, A. S. *J. Microelectromech. Syst.* **2010**, *19*, 325−337.
(33) Malcolm, A.; Wright, S.; Syms, R. R. A.; Moseley, R. W.; O' Prey, S.; Dash, N.; Pegus, A.; Crichton, E.; Hong, G.; Holmes, A. S.; Finlay, A.; Edwards, P.; Hamilton, S. E.; Welch, C. J. *Rapid Commun. Mass Spectrom.* **2011**, *25*, 3281−3288.
(34) Malcolm, A.; Wright, S.; Syms, R. R. A.; Dash, N.; Schwab, M.-A.; Finlay, A. *Anal. Chem.* **2010**, *82*, 1751−1758.
(35) Soler, C.; Mañes, J.; Picó, Y. *J. Chromatogr. A* **2005**, *1067*, 115−125.
(36) Ramanathan, R.; Çömezoğlu, S. N.; Humphreys, W. G. *Using Mass Spectrometry For Drug Metabolism Studies*, 2nd ed.; Korfmacher, W. A., Ed.; CRC Press: Boca Raton, FL, 2010; Chapter 5.
(37) Clarke, N. J.; Rindgen, D.; Korfmacher, W. A.; Cox, K. A. *Anal. Chem.* **2001**, *73*, 430A−439A.
(38) Hakala, K. S.; Kostiainen, R.; Ketola, R. A. *Rapid Commun. Mass Spectrom.* **2006**, *20*, 2081−2090.
(39) Wright, S.; Syms, R. R. A.; Moseley, R.; Hong, G.; O'Prey, S.; Boxford, W. E.; Dash, N.; Edwards, P. *J. Microelectromech. Syst.* **2010**, *19*, 1430−1443.
(40) Syms, R. R. A.; Zou, H.; Bardwell, M.; Schwab, M.-A. *J. Micromech. Microeng.* **2007**, *17*, 1567−1574.
(41) Borman, S. *Chem. Eng. News* **2006**, *84*, 45−51.
(42) Javahery, G.; Thomson, B. *J. Am. Soc. Mass Spectrom.* **1997**, *8*, 697−702.
(43) Mansoori, B. A.; Dyer, E. W.; Lock, C. M.; Bateman, K.; Boyd, R. K.; Thomson, B. A. *J. Am. Soc. Mass Spectrom.* **1998**, *9*, 775−788.
(44) Lock, C. M.; Dyer, E. *Rapid Commun. Mass Spectrom.* **1999**, *13*, 432−448.
(45) Loboda, A.; Krutchinsky, A.; Loboda, O.; McNabb, J.; Spicer, V.; Ens, W.; Standing, K. *Eur. J. Mass Spectrom.* **2000**, *6*, 531−536.
(46) Dodonov, A.; Kozlovsky, V.; Loboda, A.; Raznikov, V.; Sulimenkov, I.; Tolmachev, A.; Kraft, A.; Wollnik, H. *Rapid Commun. Mass Spectrom.* **1997**, *11*, 1649−1656.
(47) Anastassiades, M.; Lehotay, S. J.; Štajnbaher, D.; Schenck, F. *J. AOAC Int.* **2003**, *86*, 412−431.
(48) Hopley, C.; Bristow, T.; Lubben, A.; Simpson, A.; Bull, E.; Klagkou, K.; Herniman, J.; Langley, J. *Rapid Commun. Mass Spectrom.* **2008**, *22*, 1779−1786.
(49) Thomson, B. A.; Douglas, D. J.; Corr, J. J.; Hager, J. W.; Joliffe, C. L. *Anal. Chem.* **1995**, *67*, 1696−1704.
(50) Douglas, D. J.; French, J. B. *J. Am. Soc. Mass Spectrom.* **1992**, *3*, 398−408.
(51) Morris, M.; Thibault, P.; Boyd, R. K. *J. Am. Soc. Mass Spectrom.* **1994**, *5*, 1042−1063.
(52) Lock, C. M.; Dyer, E. W. *Rapid Commun. Mass Spectrom.* **1999**, *13*, 422−431.
(53) Nieminen, A.; Huikari, J.; Jokinen, A.; Äystö, J.; Campbell, P.; Cochrane, E. C. A. *Nucl. Instrum. Meth. Phys. Res. A* **2001**, *469*, 244−253.
(54) Hang, W.; Lewis, C.; Majidi, V. *Analyst* **2003**, *128*, 273−280.
(55) Page, J. S.; Kelly, R. T.; Tang, K.; Smith, R. D. *J. Am. Soc. Mass Spectrom.* **2007**, *18*, 1582−1590.
(56) European Commission, Health and Consumer Protection Directorate-General. *Guidance Document on Analytical Quality Control and Validation Procedures for Pesticide Residues Analysis in Food and Feed*, Document No. SANCO/12571/2013, November 19, 2013.
(57) Deng, W.; Klemic, J. F.; Li, X.; Reed, M. A.; Gomez, A. *J. Aerosol Sci.* **2006**, *37*, 696−714.
(58) Hill, F. A.; Heubel, E. V.; de Leon, P. P.; Velásquez-García, L. F. *J. Microelectromech. Syst.* **2014**, *23*, 1237−1248.

DOI: 10.1021/acs.analchem.5b00311
Anal. Chem. 2015, 87, 3115−3122